Comprehensive Physical Commutation Characteristic Analysis and Test of Hybrid Line Commutated Converter Based on Physics Compact Model of IGCT

Zhanqing Yu, *Member, IEEE*, Zongze Wang, Chaoqun Xu, Xuan Zhou, Zhengyu Chen, Chunpin Ren, and Rong Zeng, *Senior Member, IEEE*

***Abstract*—In order to mitigate commutation failure of high voltage direct current (HVdc) system, a novel hybrid line commutated converter (H-LCC) based on integrated gate commutated thyristor (IGCT) and thyristor has been proposed. To verify the proposed scheme's effectiveness and correctness, the physics-based compact model of reverse blocking IGCT (RB-IGCT) and physics-based model of thyristor are established in this article. By comparing the features of physics-based model with other simulation methods, it can be observed that the former has obvious advantages. On the basis, a simulation study of proposed H-LCC based on physics compact model of RB-IGCT and physics-based model of thyristor is conducted to analyze the physical commutation characteristics comprehensively, which is verified by equivalent commutation tests. The H-LCC can mitigate commutation failure of HVdc effectively and physics-based model of H-LCC is expected to be applied in the simulation of dc grid equipment and provide reference for commutation characteristics analysis and snubber parameter optimization that need rapid and multiple simulations.**

***Index Terms*—Commutation characteristic, IGCT, line commutated converter, physics-based compact model, thyristor.**

I. Introduction

THE line commutated converter based high voltage direct current (LCC-HVdc) system has become a promising solution for long-distance and large-capacity power transmission. It has advantages of low power loss, low manufacturing cost, and reliable operation [1], [2], [3]. However, the outstanding disadvantage of LCC-HVdc is that commutation failure may occur. It will influence the safe and stable operation of power grid when commutation failure occurs [4], [5], [6]. Thus, a novel hybrid line commutated converter (H-LCC) based on integrated gate commutated thyristor (IGCT) has been proposed in [7]. The topology structure of H-LCC is presented in Fig. 1. It utilizes reverse blocking IGCT (RB-IGCT) and thyristor in one bridge arm to form new hybrid commutation characteristic. The physical commutation characteristics including voltage establishment characteristic and current transferring characteristic are of great importance for engineering application of H-LCC and need to be investigated in depth. Therefore, the physical characteristic analysis of H-LCC should be on the basis of physics model simulation of high-power devices.

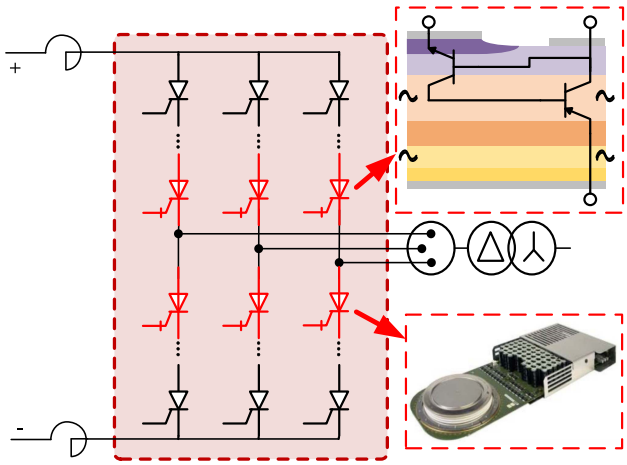

Fig. 1. H-LCC topology structure and applying power devices.

At present, due to different analysis requirements, various simulation models of high-power devices have been proposed and have different accuracy and speed. The analysis models, which have been reported can be divided into five levels [8], ideal switch model, circuit element model, lumped charge model, physics-based compact model, and finite element simulation model.

The ideal switch model and circuit element model do not involve the physical mechanism of power device, so they can not accurately describe the dynamic characteristics of the device

Manuscript received 28 July 2022; accepted 7 October 2022. Date of publication 10 October 2022; date of current version 18 November 2022. This work was supported in part by Integration Projects of National Natural Science Foundation of China-State Grid Joint Fund for Smart Grid under Grant U2166602 and in part by the National Natural Science Foundation of China under Grant 51922062. Recommended for publication by Associate Editor D. Dujic. *(Corresponding author: Chaoqun Xu.)*

Zhanqing Yu, Zongze Wang, Chaoqun Xu, Xuan Zhou, Chunpin Ren, and Rong Zeng are with the Department of Electrical Engineering, Tsinghua University, Beijing 100084, China (e-mail: yzq@tsinghua.sedu.cn; zzwang132@163.com; xucq18@mails.tsinghua.edu.cn; zhouxuan12@tsinghua.org.cn; 18810-903251@163.com; zengrong@tsinghua.edu.cn).

Zhengyu Chen is with the Sichuan Energy Internet Research Institute, Tsinghua University, Beijing 100084, China (e-mail: chenzhen14@tsinghua.org.cn).

Color versions of one or more figures in this article are available at https://doi.org/10.1109/TPEL.2022.3213490.

Digital Object Identifier 10.1109/TPEL.2022.3213490

[9], [10], [11], [12], [13]. Both the lumped charge model and the physics compact model are based on the simplified physical equation of the device. The latter uses the bipolar diffusion equation to replace the lumped charge description, which has higher accuracy and is more suitable for circuit level simulation [14], [15], [16], [17], [18], [19]. The finite element model solves the basically complete semiconductor equations, and the physical description of the device is the most accurate, but the calculation speed is slow.

Relevant studies are mainly focused on 2 and asymmetrical IGCT. Two-dimensional (2-D) and 3-D simulation for asymmetrical IGCT devices are proposed in [20] and [21], adopting a complete bipolar diffusion equation and considering thermal model and ionization model. However, its calculation speed is too slow and not for RB-IGCT. Thus, it is not appropriate for H-LCC analysis. A physics-based compact asymmetrical IGCT model is proposed in [17], and introduced Fourier method to accelerate the solution. However, the doping structure and physical mechanism of RB-IGCT are different from asymmetrical IGCT device, and the relevant asymmetrical IGCT model cannot be directly transferred to RB-IGCT. In particular, the reverse recovery dynamic process of RB-IGCT is more complex. It is urgent to establish a high-precision physics-based simulation model of RB-IGCT, which is very important for physical characteristic analysis of H-LCC.

Thus, in this article, the physics-based compact model of RB-IGCT and physics-based model of thyristor are established. Based on physics simulation methods, the advantages of characteristics analysis are extracted by comparison with ideal switch model and finite element model. Furthermore, the physical commutation characteristics of H-LCC are analyzed in detail and verified by tests. The physical commutation characteristics of H-LCC are proven to be of correctness and effectiveness for prosperous engineering application.

II. Proposed Physics-Based Simulation Models

To analyze the comprehensive physical commutation characteristics of the proposed H-LCC, the high-precision models of RB-IGCT and thyristor are built in this section, including physics-based compact model of RB-IGCT and physics-based model of thyristor.

A. Physics-Based Compact Model of RB-IGCT With Double Depletion Layers

As mentioned in the last section, a physics-based compact asymmetrical IGCT model is proposed in [17] and [23], like Fig. 2(a), which includes the modeling of N^+-emitter, P-base, J_2 depletion layer, carrier storage region (CSR) in N-base, N-buffer, and P^+-emitter. On the basis of it, the anode P-base region replaces the N-buffer region in an RB-IGCT chip, as shown in Fig. 2(b). Thus, the P-N junction J_1 needs to be considered, and the two adjacent areas, N-base and P^--anode regions, need to be reconstructed.

J_1 depletion region causes different boundary conditions of CSR in the N-base region. The positions of the moving boundaries x_1, x_2 (as shown in Fig. 2) are determined by the widths W_{d1} and W_{d2} of depletion layers of J_1 and J_2 layers. The widths

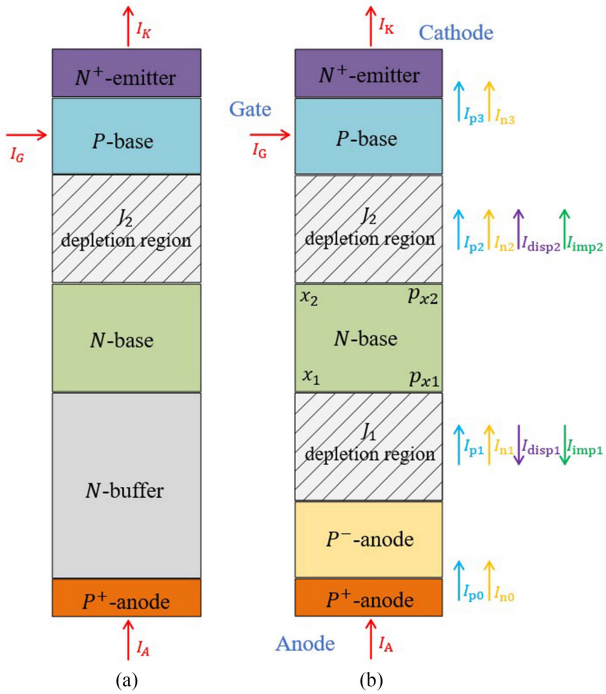

Fig. 2. Diagram of physical modelling comparison of IGCT. (a) Asymmetrical IGCT (b) RB-IGCT.

and boundaries can be derived as carrier injection conditions (1) and (2) in [17], where E_{J1}, E_{J2} are the electric fields inside the depletion layers, $\varepsilon_{\mathrm{Si}}$ is the dielectric constant of silicon, N_{Nb} is the doping density of N-base region, v_{sat} is the saturation velocity, and W_{Nb} is the width of N-base region. The essence is that the drift charge generates the electric field of the depletion layer. It is considered that impact ionization only occurs in a small area near J_1 and J_2, so the impact of impact ionization on the overall electric field distribution is ignored. Then, W_{d1} and W_{d2} are calculated from the relationship between the electric field intensity and the voltage

$$\begin{cases} E_{\mathrm{J1}} = \frac{qN_{\mathrm{Nb}}}{\varepsilon_{\mathrm{Si}}} + \frac{|I_{\mathrm{p1}}|}{\varepsilon_{\mathrm{Si}} A v_{\mathrm{sat}}} - \frac{|I_{\mathrm{imp1}}|}{\varepsilon_{\mathrm{Si}} A v_{\mathrm{sat}}} \\ W_{\mathrm{d1}} = \sqrt{\frac{2V_{\mathrm{d1}}}{E_{\mathrm{J1}}}} \\ x_1 = W_{\mathrm{d1}} \end{cases} \tag{1}$$

$$\begin{cases} E_{\mathrm{J2}} = \frac{qN_{\mathrm{Nb}}}{\varepsilon_{\mathrm{Si}}} + \frac{|I_{\mathrm{p2}}|}{\varepsilon_{\mathrm{Si}} A v_{\mathrm{sat}}} - \frac{|I_{\mathrm{imp2}}|}{\varepsilon_{\mathrm{Si}} A v_{\mathrm{sat}}} \\ W_{\mathrm{d2}} = \sqrt{\frac{2V_{\mathrm{d2}}}{E_{\mathrm{J2}}}} \\ x_2 = W_{\mathrm{Nb}} - W_{\mathrm{d2}}. \end{cases} \tag{2}$$

The voltages of depletion layers, V_{d1} and V_{d2}, can be derived using feedback from the boundary carrier density, p_{x1} and p_{x2}, as presented in (3) and (4) in [22] and [23], where F is a constant. These equations establish the relationship between carrier and voltage. F is an artificially introduced correction factor, which has no practical physical significance, but can greatly improve the simulation speed

$$V_{\mathrm{d1}} = \begin{cases} 0 & p_{\mathrm{x1}} > 0 \\ -Fp_{\mathrm{x1}} & p_{\mathrm{x1}} \le 0 \end{cases} \tag{3}$$

$$V_{\mathrm{d2}} = \begin{cases} 0 & p_{\mathrm{x2}} > 0 \\ -Fp_{\mathrm{x2}} & p_{\mathrm{x2}} \le 0 \end{cases} \tag{4}$$

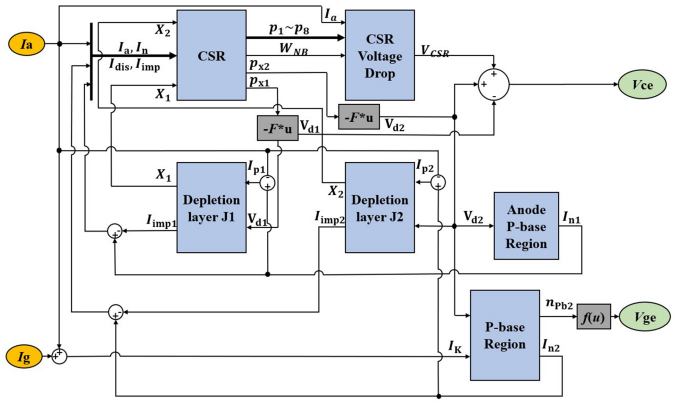

Fig. 3. Implementation of proposed physics-based compact model of RB-IGCT in MATLAB/Simulink.

$$\begin{cases} \frac{\partial p(x,t)}{\partial t} = D\frac{\partial^2 p(x,t)}{\partial x^2} - \frac{p(x,t)}{\tau_H} \\ D = \frac{2D_{\rm n}D_{\rm p}}{D_{\rm n}+D_{\rm p}} \\ \left.\frac{\partial p}{\partial x}\right|_{x1} = \frac{1}{2qA}\left(\frac{I_{\rm n1}-I_{\rm imp1}}{D_{\rm n}} - \frac{I_{\rm p1}}{D_{\rm p}}\right) \\ \left.\frac{\partial p}{\partial x}\right|_{x2} = \frac{1}{2qA}\left(\frac{I_{\rm n2}-I_{\rm imp2}}{D_{\rm n}} - \frac{I_{\rm p2}}{D_{\rm p}}\right). \end{cases} \tag{5}$$

The CSR in *N*-base region is considered in high injection level, whose boundary carrier equation will change from single depletion layer to double. Thus, the excess carrier density can be described as (5) in [17] and [23]. It is a diffusion equation considering double boundary conditions. At the same time, the ADE method is used to ignore the convection equation and improves the simulation speed. In addition to some constant coefficients, the carrier concentration and thickness of each layer in the model need to be adjusted according to the actual device, which should be given by the device designer. Therefore, device design optimization and physics-based compact model simulation are complementary.

The compact model of RB-IGCT is implemented in MATLAB/Simulink and the outline block diagram of the model is shown in Fig. 3. The modules and circuits in Fig. 3 represent different layers and carrier relationship between them in Fig. 2 respectively, adding J_1 region and anode P^- region compared with the asymmetric IGCT model in [17]. When the current passes through, the carrier concentration is positive, so the width of the depletion layers is 0. When the device is turned OFF, $I_{\rm g}$ first becomes negative, resulting in negative $V_{\rm ge}$, which causes the current to reverse from the cathode to the gate, and the J_2 between the gate and cathode will establish a positive voltage, thus causing $I_{\rm a}$ to decrease to 0. Using this physics-based compact model of RB-IGCT, it can not only be seen what the voltage and current of this model are, but also how the carrier moves through RB-IGCT chip by extracting the change of p and x in Fig. 3, which will play a great role in analyzing the physical characteristics of H-LCC in different processes.

B. Physics-Based Model of Thyristor With Controlled Reverse Recovery Current

In the simulation of H-LCC converter, the reverse recovery current is a significant characteristic of thyristor, which affects the current and voltage on the devices (including RB-IGCTs and thyristors) in the commutation process. The physics-based model of thyristor, compared with ideal switch, shows better performance on reverse recovery characteristics. As shown in Fig. 4, the physics-based thyristor model consists of main part, trigger circuit, where the voltage of $R_{\rm g}$ controls ON and OFF of S_1, and current source generator. This model has the same performance as ideal switch in the process of turning ON, but when the current is reduced to 0, it works differently.

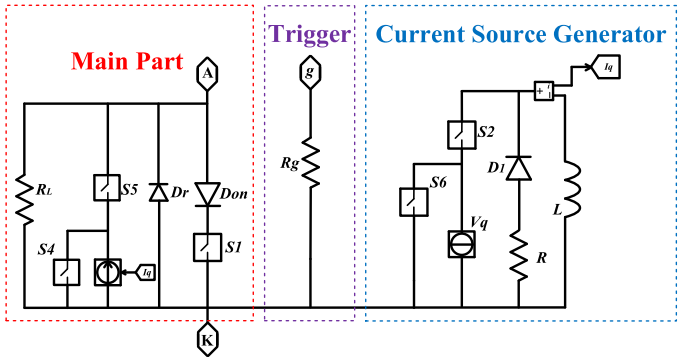

Fig. 4. Schematic diagram of physics-based simulation model of thyristor.

When the current through anode and cathode decreases to 0, the current source generator begins to work. The controlled voltage source $V_{\rm q}$ charges the inductor L when S_2 is ON and S_6 is OFF, and then L is discharged through the resistance R and the diode D_1 with S_2 OFF and S_6 ON. With the control of S_4, S_5, and $I_{\rm q}$, the reverse parallel controlled current source output a reverse recovery current through anode. The waveform of reverse recovery current, including di/dt and reverse recovery time $T_{\rm rr}$, depends on $V_{\rm q}$, L, R and turn-ON time of S_2. Besides, $R_{\rm L}$, $D_{\rm r}$, and $D_{\rm on}$ mean OFF state resistance, reverse maximum withstand voltage, and unidirectional current characteristics.

Compared with RB-IGCT, thyristors do not have the ability to actively turn OFF current. They only reflect the characteristics of reverse recovery in H-LCC topology, so more complex models are not required. The thyristor model proposed in this chapter has advantage of fast calculation speed, and the reverse recovery characteristics can be adjusted according to the measured values.

Connecting the physics-based compact model of RB-IGCT and the physics-based model of thyristor in series, a new equivalent model of H-LCC bridge can be obtained. Both models adopt the optimization scheme that can show their characteristics, so the simulation speed will be faster than finite-element method, which can be of great help to the parameter design of the H-LCC. H-LCC model can help analyzing the characteristics of both thyristors and IGCTs during the commutation process under different conditions. The reverse recovery characteristics of the actual thyristor and RB-IGCT are always different, and the difference will be reflected in the recovery time, which will affect the dynamic voltage sharing between devices. It is necessary to keep the difference of reverse recovery characteristics in the simulation, and observe the voltage distribution with different recovery characteristics through simulation, so as to provide reference for the engineering application of devices.

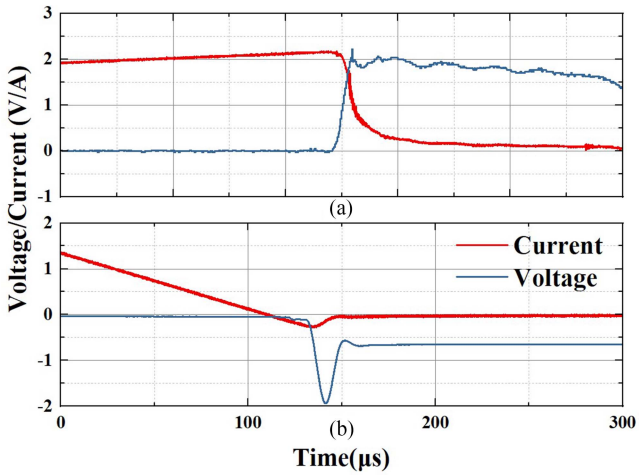

Fig. 5. Test waveforms of RB-IGCT. (a) Triggered turn-OFF process. (b) Reverse blocking process.

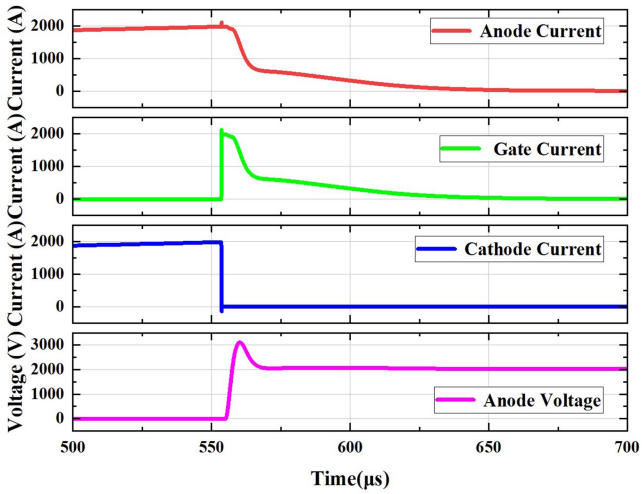

Fig. 6. Simulation waveforms of triggered turn-off process under forward voltage of RB-IGCT.

III. Comprehensive Characterization of Physics-Based Method

A. Physics-Based Method Verification by Single-Pulse Test

In the application of RB-IGCT and thyristor, the states of devices are divided into steady state, including ON and OFF, and transient state, including turning ON, turning OFF (only for RB-IGCT) and reverse blocking. Among these processes, steady state and turning ON process are simple, without complex transient process, so turning OFF and reverse blocking processes deserve more attention. Fig. 5 shows the typical turning OFF and reverse blocking experimental waveforms of IGCT. The main characteristics include turning OFF speed, trailing current, reverse recovery current, and overvoltage. It should be verified that the physics-based model has those characteristics by single-pulse test. Therefore, the parameters of testing RB-IGCT compact model are designed for a 6.5 kV RB-IGCT. Turning OFF process under forward voltage and reverse blocking process under reverse voltage are simulated in MATLAB/Simulink.

The simulation waveform of turn-OFF process under forward voltage is shown as Fig. 6. The RB-IGCT is triggered to turn off at 550 μs, when the current is 2000 A and anode voltage is 2000 V. It can be observed that the cathode current is transferred to the gate rapidly, anode voltage is increasing while anode current is decreasing, and there is the tail current as well. The simulation results are in good agreement with experimental waveform abovementioned, which proves the effectiveness of the physics-based compact model of RB-IGCT during turn-OFF under forward voltage.

Observe the reverse blocking characteristics of RB-IGCT compact model and physics-based thyristor model. The simulation waveform of reverse blocking process under reverse voltage is shown as Fig. 7. There is obvious reverse recovery current before the voltage is built up. Besides, the characteristics can be accurately extracted by adjusting the parameters.

Considering H-LCC working condition, RB-IGCT needs to meet the ability to turn OFF 5500 A under the arrester voltage

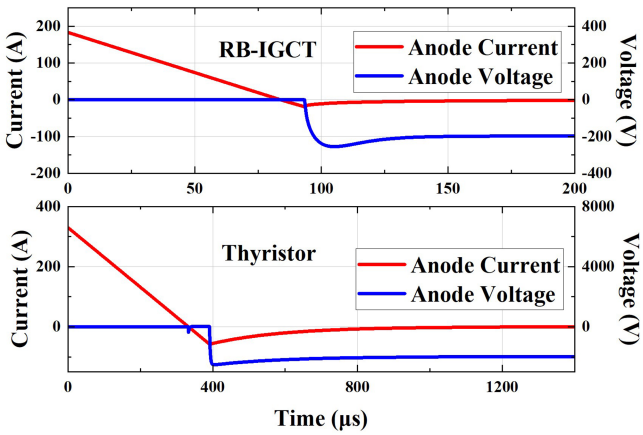

Fig. 7. Simulation waveforms of reverse blocking process under reverse voltage of RB-IGCT and thyristor.

clamping of about 6000 V. At the same time, the snubber capacitor commonly used in the system is 1.6 to 2.2 μF, with a small adjustable range, which does not affect the turning-OFF process greatly. Therefore, authors pay more attention to turning-OFF under different snubber resistors. The following Figs. 8 and 9 are waveforms of turning-OFF 5500 A under 1 Ω and 36 Ω snubber resistance, respectively. It can be observed in Fig. 8 that after the cutoff command is issued, the snubber branch works first, so the IGCT current I_{IGCT} first drops. When the voltage rises but the arrester branch current I_{MOV} has not yet appeared, the current will be switched back to the IGCT. Only when the voltage rises to the starting value of arrester, I_{IGCT} will be gradually transferred to I_{MOV}, accompanied by the tailing current. It can be observed from Fig. 9 that when the snubber resistance increases to 36 Ω, the snubber effect almost disappears. Therefore, after the cutoff command is issued, I_{IGCT} will not decrease immediately. I_{IGCT} can only be transferred to I_{MOV} after the voltage rises to the starting value of the arrester. The simulation results are in good agreement with the experimental results.

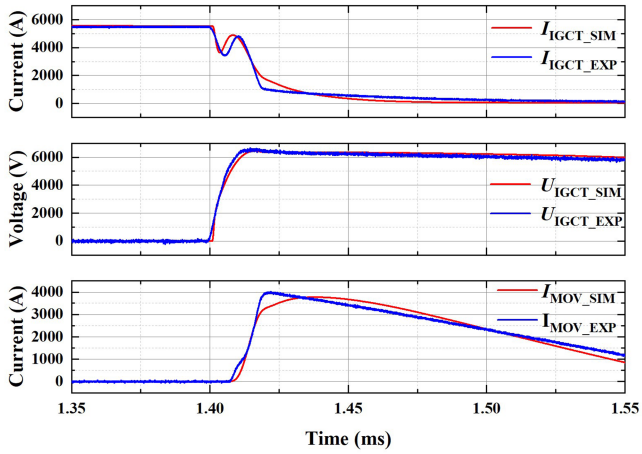

Fig. 8. RB-IGCT turning-off with 1 Ω snubber resistance.

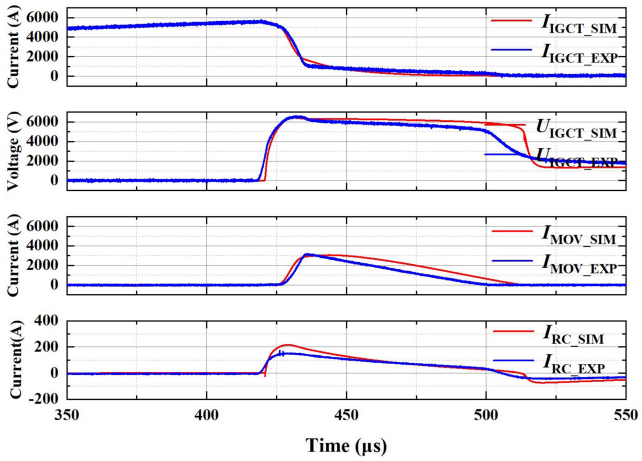

Fig. 9. RB-IGCT turning-OFF with 36 Ω snubber resistance.

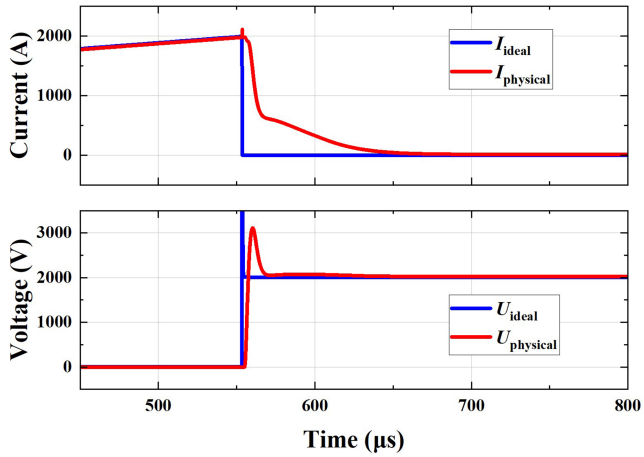

Fig. 10. Simulation waveforms of ideal switch and physics-based method.

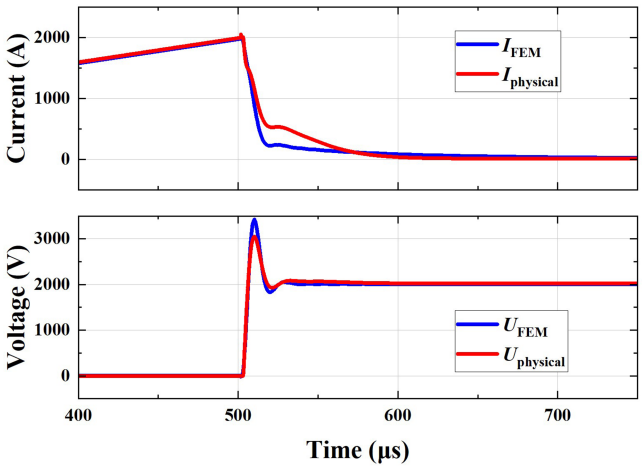

Fig. 11. Simulation waveforms of finite-element method and physics-based method.

B. Physics-Based Method Advantages

On the basis of single-pulse test, physics-based methods, including RB-IGCT compact model and thyristor model, are verified. Compared with the other simulation methods, such as simpler ideal switch model and more complex finite-element model, physics-based models have incomparable advantages.

Ideal switch model is generally used for large-scale systematic simulation design and multidevice system control simulation due to its great advantage in computing speed. The compact model can reflect some physical characteristics and has the advantage of good computing speed. It is generally used in circuit parameter and system parameter design, and has good applications in device driving design, topology design and thermal characteristic calculation. The finite element model is very accurate in the extraction of physical characteristics, which is mainly used for the prediction of device failure and aging, as well as the accurate structure design of devices. But due to the long simulation time, it is not suitable for circuit and system simulation.

There are only two states of the ideal switch, the ON state with a voltage drop and the OFF state with infinite impedance. The transition time between the two states is 0 or depends on the simulation step to facilitate numerical conversion, as shown in Fig. 10. The finite element method is very precise for the calculation of physical processes in semiconductors, and the convection diffusion (6) is used for the motion of carriers, where φ means the parameter to be solved, u means moving speed, α is thermal diffusivity. The equation can be decomposed into convection (7) and diffusion (8). Compared with the diffusion equation, the calculation of convection equation is much slower, which is also a key factor limiting the speed of finite element simulation. Compact model is improved to this point. It only solves the diffusion equation, does not solve the convection equation, but uses the mathematical method for equivalence, which can greatly improve the simulation speed in the case of similar accuracy, as shown in Fig. 11

$$\frac{\partial \varphi}{\partial t} + u\frac{\partial \varphi}{\partial x} = \alpha \frac{\partial^2 \varphi}{\partial x^2} \tag{6}$$

$$\frac{\partial \varphi}{\partial t} + u\frac{\partial \varphi}{\partial x} = 0 \tag{7}$$

$$\frac{\partial \varphi}{\partial t} = \alpha \frac{\partial^2 \varphi}{\partial x^2}. \tag{8}$$

TABLE I
COMPARISON OF DIFFERENT MODELS

Model	Ideal switch	Physics-based method	Finite-element method
Time	Seconds	Seconds to minutes	Hours to days
Accuracy	Inaccurate	Relatively accurate	Accurate
Application	System	Equipment	Device
Carrier behavior	No	Yes	Yes

The simulation step of compact model is adaptive, so its calculation results are more robust. The accuracy of the ideal model depends on the simulation step size, which is not true. Meanwhile, with accurate physical characteristics, compact model can be used to assist in the analysis of safe operating areas and tap the potential of devices. Compared with the finite element model, the computation speed of compact model is nearly 1000 times faster. During the simulation of scanning *RC* parameters required by the project to extract the best combination, it is often necessary to simulate dozens of groups of parameters. The workload can be completed in several hours by compact model, and the finite element method may take several weeks. Due to the huge amount of computation, finite element method often needs high-performance servers, while compact model has a moderate amount of computation, which will greatly reduce the demand for computing equipment.

Table I sorts out the comparison of the three models from various aspects. The physics-basic model has obvious advantages over the other two models.

C. Applications of Physics-Based Compact Model

First, the physics-based compact model can help to analyze the safe operating area of RB-IGCT cutoff process. As shown in Fig. 12, (1), (2), and (3) are RB-IGCT cutoff process curves under different snubber parameters by physics-based compact model. Among them, Fig. 12 (1) shows that the larger the clamping voltage of the arrester is, the larger the area of the cutoff curve will be, which will increase the risk of cutoff failure. Fig. 12 (2) shows the scanning of snubber resistance. The smaller the snubber resistance value is, the smaller the turn-OFF curve area is. Fig. 12 (3) shows the scanning of snubber capacitance. The larger the snubber capacitance value is, the better the snubber effect will be, so as to reduce the risk of cutoff damage. Predicting the risk in advance by means of simulation can reduce the possibility of experimental damage and save experimental costs.

Second, the physics-based compact model can be used to extract the internal carrier movement characteristics of RB-IGCT. As shown in Fig. 13, when the bus voltage or turn-OFF current are different, there are differences in the carrier distribution and junction formation process of RB-IGCT. Fig. 14 shows that the smaller the resistance or the higher the capacitance, the stronger the snubber effect and the smoother the curve. Fig. 15 indicates that the current change rate plays an important role in the reverse blocking process. The carrier characteristics can

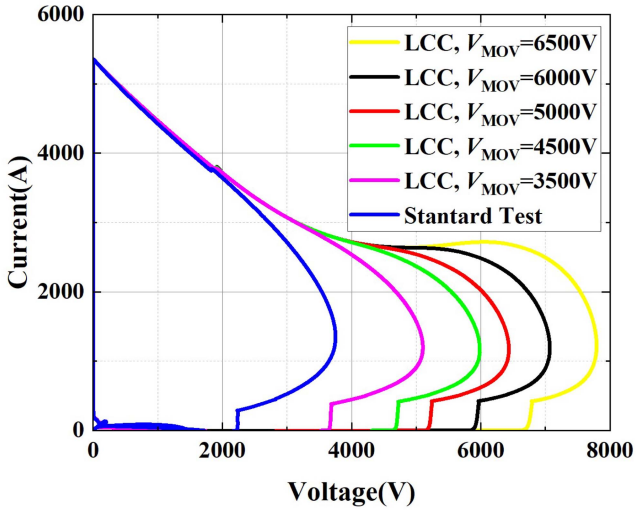

(a)

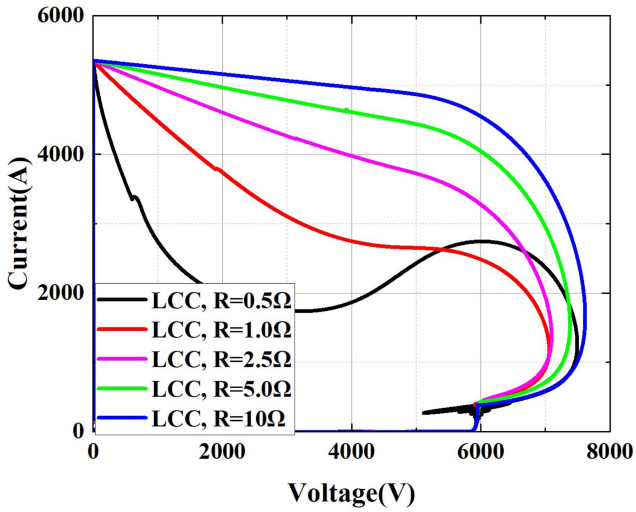

(b)

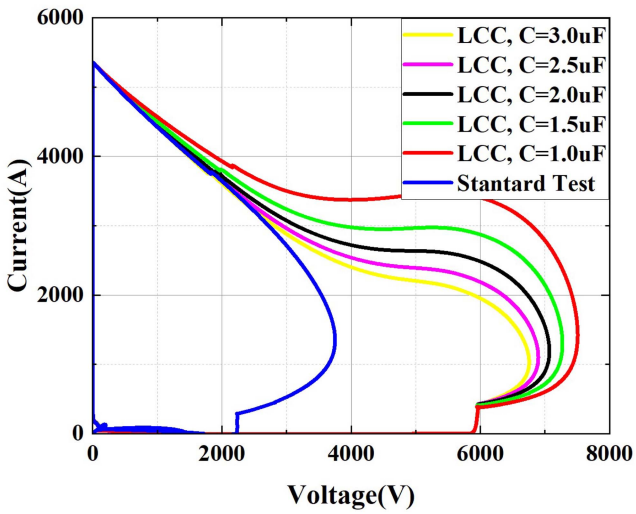

(c)

Fig. 12. U-I curve of cutoff process under different snubber parameters. (a) With different MOV clamping parameters. (b) With different snubber resistances. (c) With different snubber capacitances.

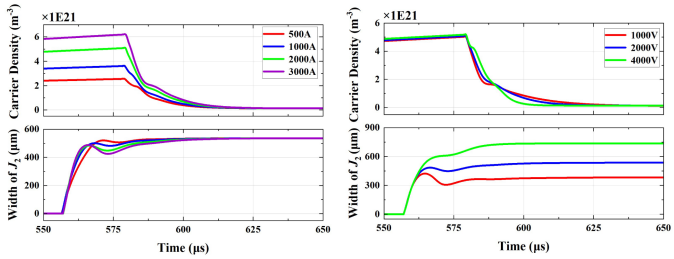

Fig. 13. Carrier distribution of J_1 and the width of J_2 during turn-OFF process with different current and voltage. (a) Under different anode currents. (b) Under different DC-bus voltages.

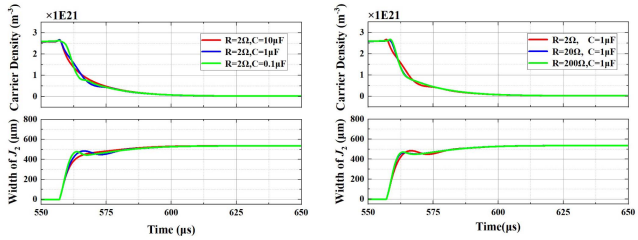

Fig. 14. Carrier distribution of J_1 and the width of J_2 during turn-OFF process with different snubber parameters. (a) With different snubber capacitances. (b) With different snubber resistances.

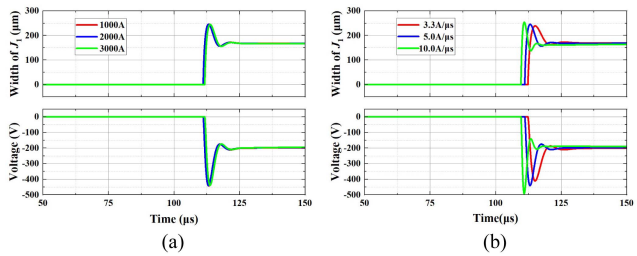

Fig. 15. Width of J_1 and the voltage of J_1 during reverse blocking process with different current and its change rate. (a) Under different anode currents. (b) Under different di/dt.

be extracted quickly and accurately by using the physics-based compact model, which is convenient for more physical analysis.

In addition, the physics-based compact model can build a bridge between circuit simulation and the physical process of devices to help analyze the physical characteristics of LCC commutation process, which will be described in Section IV.

IV. Comprehensive Physical Commutation Characteristic Analysis and Test

In the H-LCC converter, there are two different working conditions. On one hand, when a slight fault occurs in the ac grid, the voltage drop amplitude is small. At this time, the current on the converter valve can decrease to 0, as shown in Fig. 16(1), but the voltage will become positive during the recovery period of the thyristor. If there are only thyristors, they will be retriggered, resulting in commutation failure. But in H-LCC, due to the shorter reverse recovery time, RB-IGCTs can withstand the positive voltage preferentially to avoid commutation failure caused, called recovery enhanced characteristic. In this working

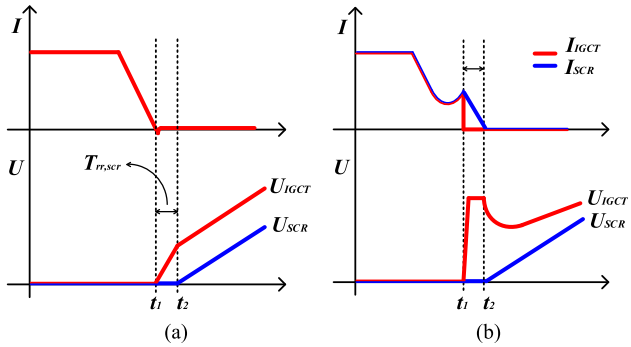

Fig. 16. Different working conditions in H-LCC. (a) Recovery enhanced characteristic. (b) Commutation enhanced characteristic.

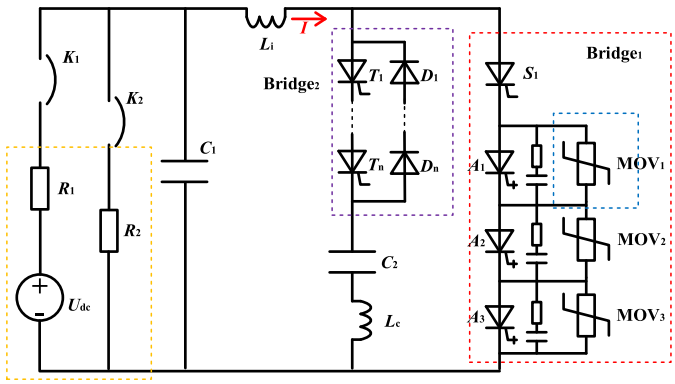

Fig. 17. Equivalent commutation test circuit.

condition, RB-IGCTs take the forward voltage for about 400 μs, which is longer than the reverse recovery time of thyristors. After this, thyristors begin to withstand voltage.

On the other hand, when a serious fault occurs in the ac grid, the voltage may directly drop to 0. At this time, the current on the converter valve may rise rapidly, and the continuous commutation failure will occur in the LCC system, resulting in dc locking and large losses. In order to avoid continuous commutation failure, RB-IGCTs are used to turn OFF the current, as shown in Fig. 16(2). When turning OFF RB-IGCTs, current transfers from switches to the arrester, resulting in a high voltage of RB-IGCTs and the decrease of thyristor's current. During the time between t_1 and t_2, the voltage is the residual voltage of arrester. Thyristor begins to withstand voltage after the current becomes to 0 and the reverse recovery is completed. The current of bridge$_1$ can be commutated to bridge$_2$, which is called commutation enhanced characteristic.

For the recovery enhancement process, the most important thing is to reflect the role of RB-IGCT in mitigating commutation failure with shorter recovery time. Obviously, the ideal device cannot complete this job. For the commutation enhancement process, more attention should be paid to the electrical stress on different components during RB-IGCT cutoff, so the cutoff process should be more physical. The physics-based model can complete the simulation of these two working conditions with high accuracy. At the same time, the simulation speed is fast so that it can be used in multiple simulation.

The test platform is built and circuit is shown in Fig. 17. It is the hybrid converter of thyristor and RB-IGCTs in the red dotted line with snubber *RC* and arrester, where S_1 represents a thyristor and A_1–A_3 represent RB-IGCTs. In LCC condition and in the demand of voltage balance, snubber *RC* is indispensable. And when turning OFF, arresters are necessary to limit overvoltage and absorb energy, without which IGCTs will get overvoltage breakdown. The starting voltage of arrester must be higher than the maximum value during normal operation, and the protection voltage must be lower than the withstand peak value of IGCTs. Bridge$_2$ is the auxiliary switch to assist commutation of bridge$_1$, which is composed of thyristors and diodes. There is the charging and discharging circuit of C_1 in the yellow dotted line. By controlling switches and the voltages on two capacitors C_1 and C_2, two different working conditions of H-LCC can be realized.

In the following tests and analysis, the recovery enhanced characteristic and commutation enhanced characteristic are studied.

A. *Recovery Enhanced Characteristic Analysis and Test*

The main reason for the commutation failure of LCC is that thyristors withstand positive voltage in advance due to the insufficient extinction angle. Under most conditions, current flowing through thyristors can decrease to 0.

It can be simulated using the circuit in Fig. 17. First, charge the capacitors C_1 and C_2 through the dc source, and then turn ON the switches on bridge$_1$ to discharge the capacitor C_1 to the inductor L_i. Next turn ON the switches on bridge$_2$ and use the resonance of C_2 and L_c to commutate the current on bridge$_1$ to the bridge$_2$. By controlling the capacitor voltage and switching time, the devices can bear the positive voltage immediately after the current is reduced to 0, so as to observe the recovery enhancement characteristic.

Fig. 18 shows the experimental and simulation results, which are consistent in trend. When the current drops to 0, IGCTs preferentially bear the reverse voltage, which indicates that the reverse recovery time of IGCT is shorter than that of thyristor. After voltage turns positive, IGCTs also take priority to bear it, which indicates that IGCT has shorter forward recovery time and is conducive to resisting commutation failure. When the thyristor voltage begins to rise, the IGCTs' voltage rise rate decreases. Of course, there are some differences between the experimental and simulation waveforms because the parameters in the simulation are fixed, but those in experimental are floating, such as stray parameters, manual adjustment error, and so on.

The carrier density distribution curve of carrier storage region under 4000 A is extracted from the physics-based compact model, as shown in Fig. 19, where 0 μs means the time when current decreases to 0. With the decrease of current, the carrier density shows a downward trend. The carrier density near J_1 decreases rapidly and preferentially decreases to 0. The carrier density near J_2 decreases slowly. The depletion layer is formed and extends in J_1 with the sweeping out of excess carriers first. The reverse high voltage is withstood by J_1 depletion layer. But soon when J_2 depletion layer is formed, the voltage changes to positive and is withstood by J_2.

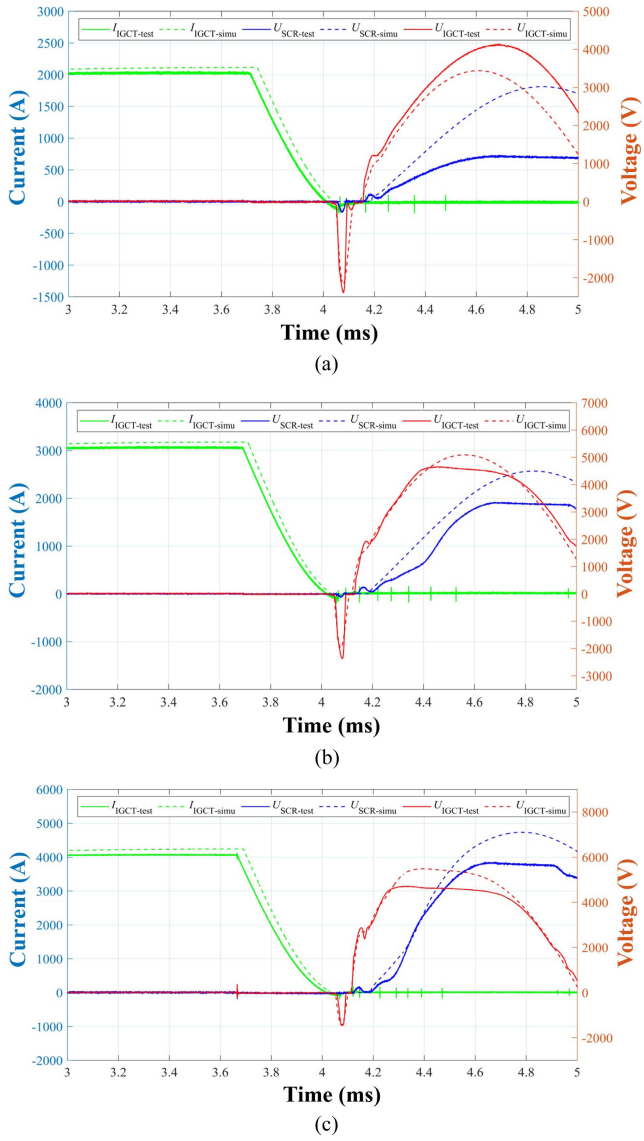

Fig. 18. Recovery enhancement waveforms of thyristor and RB-IGCTs under different current: (a) 2000 A; (b) 3000 A; (c) 4000 A.

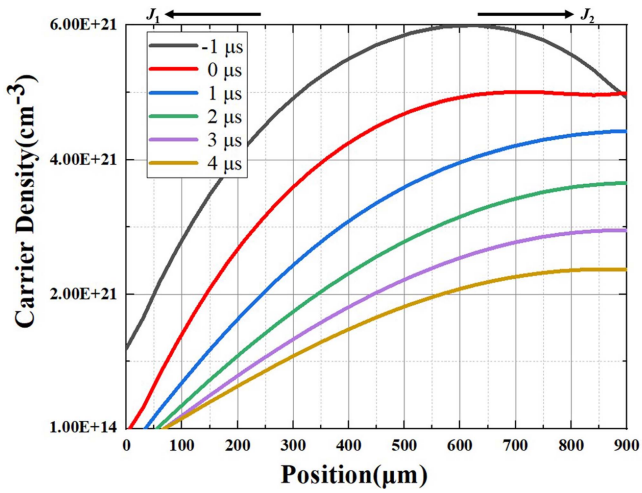

Fig. 19. Carrier density distribution variation of *N* base region during recovery enhancement of RB-IGCT.

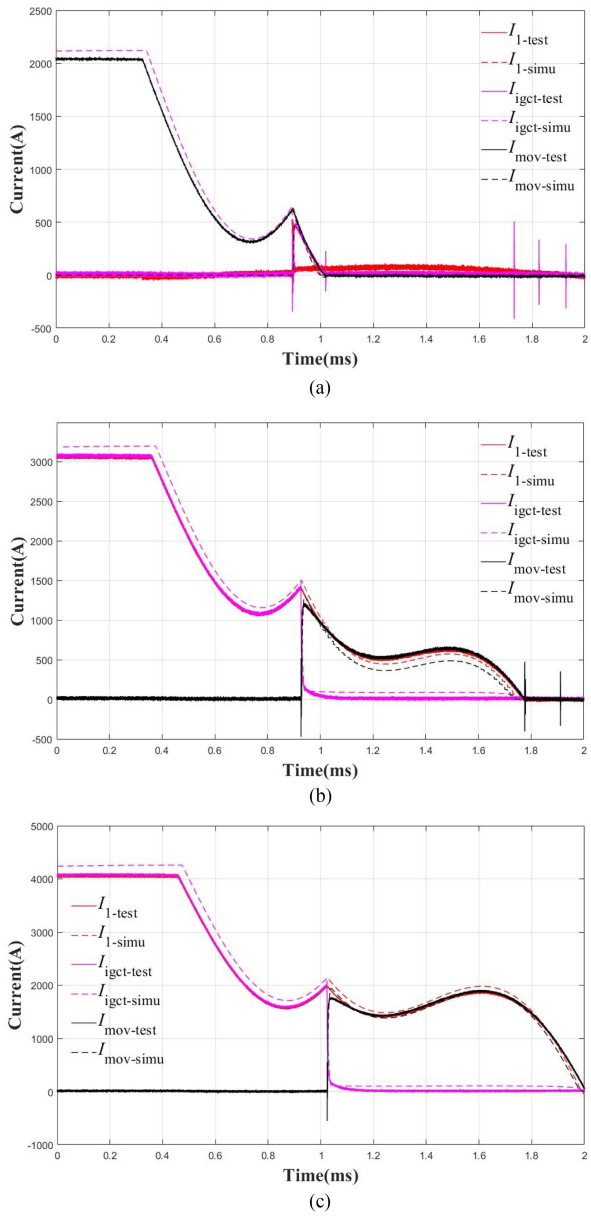

Fig. 20. Commutation enhancement waveforms under different current conditions: (a) 2000 A; (b) 3000 A; (c) 4000 A.

B. Commutation Enhanced Characteristic Analysis and Test

Under some extreme working conditions of commutation faults, the current cannot decrease to 0. It is necessary to turn OFF the current by using RB-IGCTs to force the current to be commutated to another bridge.

As can be seen from Fig. 17, there are snubber circuit and arrester connected in parallel with RB-IGCTs. When RB-IGCTs are turned OFF, the current is transferred to the snubber circuit first, then to the arresters. In the commutation enhancement, the voltage reaches the residual voltage of the arrester, which is a constant lower than the maximum withstand voltage of RB-IGCTs. Therefore, the current distribution of each branch deserves more analysis.

Fig. 20 shows the process of current transfer when IGCTs are turning OFF, where I_1 means the total current, also the current

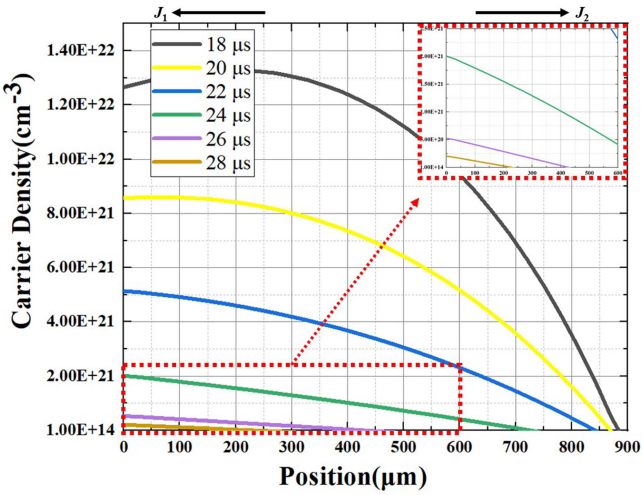

Fig. 21. Carrier density distribution variation of N base region during commutation enhancement of RB-IGCT.

of thyristor. The current on the IGCTs drops rapidly and is first transferred to the buffer circuit, too fast to be shown in Fig. 20. When the voltage reaches the operating voltage of arresters, the current is transferred to arresters, whose voltage is maintained at the residual voltage. During this process, the thyristor is always on until the current is commutated to another bridge arm. Meanwhile, with the increase of the turn-OFF current, the bus voltage also increases, but the residual voltage of the arrester remains unchanged. Therefore, the voltage on the commutation inductance will drop and the commutation time will be longer.

The carrier density distribution curve of carrier storage region around 1 ms during commutation enhancement under 2000 A is extracted from the physics-based compact model, as shown in Fig. 21. The carrier density near J_2 is quickly swept away, so that the cathode current is transferred to the gate. At this time, the forward high voltage has been established. The depletion layer is formed and extended gradually in J_2 instead of J_1 under this condition of commutation enhancement. The forward high voltage is withstood by J_2 depletion layer.

C. Beneficial Advantages

The physical commutation characteristics of proposed H-LCC, which is composed of thyristors and RB-IGCTs, are studied by tests and physics-based simulations. By analyzing the test results and simulation results, it can be concluded that the simulation results, with physics-based compact model of RB-IGCT and physics-based model of thyristor, are in good agreement with the test results, which proves the effectiveness of this physics-based method. It is especially appropriate to be used to design and simulate the parameters of the H-LCC composed of thyristors and IGCTs, and design optimized parameters of passive components.

V. Conclusion

In this article, a physics-based compact model of RB-IGCT and a physics-based model of thyristor are established. By single-pulse test, the accuracy and correctness of physics-based

methods are verified, including characteristics of triggered turn-OFF process under forward voltage of RB-IGCT, and characteristics of reverse blocking process under reverse voltage of RB-IGCT and thyristor. The physics-based methods have advantages in accuracy and simulation speed and can be applied on occasions that need rapid and multiple simulation, including commutation characteristics analysis and snubber parameter optimization. Carrier behavior analysis is conducted and shows the detailed interaction between internal behavior of devices and external electromagnetic transient characteristics. By using this physics-based methods and implementing equivalent commutation tests, the comprehensive physical commutation characteristics of proposed H-LCC are analyzed in detail. By simulations and tests, it is proved that H-LCC can mitigate commutation failure of HVdc system. And H-LCC is expected to be applied in HVdc to improve the safe and stable operation.

It is believed that the physics-based analysis methods can be further applied into dc equipment based on IGCT. And it can provide great reference for characteristics extraction and stimulate engineering applications.

REFERENCES

[1] O. E. Oni, I. E. Davidson, and K. N. I. Mbangula, "A review of LCC-HVDC and VSC-HVDC technologies and applications," in *Proc. IEEE 16th Int. Conf. Environ. Elect. Eng.*, 2016, pp. 1–7.

[2] G. Li et al., "Feasibility and reliability analysis of LCC DC grids and LCC/VSC hybrid DC grids," *IEEE Access*, vol. 7, pp. 22445–22456, 2019.

[3] H. Rao et al., "Key technologies of ultra-high voltage hybrid LCC-VSC MTDC systems," *CSEE J. Power Energy Syst.*, vol. 5, no. 3, pp. 365–373, Sep. 2019.

[4] L. Hong et al., "Analysis and improvement of the multiple controller interaction in LCC-HVDC for mitigating repetitive commutation failure," *IEEE Trans. Power Del.*, vol. 36, no. 4, pp. 1982–1991, Aug. 2021.

[5] W. Yao, C. Liu, J. Fang, X. Ai, J. Wen, and S. Cheng, "Probabilistic analysis of commutation failure in LCC-HVDC system considering the CFPREV and the initial fault voltage angle," *IEEE Trans. Power Del.*, vol. 35, no. 2, pp. 715–724, Apr. 2020.

[6] L. Hong, X. Zhou, H. Xia, Y. Liu, and A. Luo, "Mechanism and prevention of commutation failure in LCC-HVDC caused by sending end AC faults," *IEEE Trans. Power Del.*, vol. 36, no. 1, pp. 473–476, Feb. 2021.

[7] C. Xu et al., "A novel hybrid line commutated converter based on IGCT to mitigate commutation failure for high-power HVdc application," *IEEE Trans. Power Electron.*, vol. 37, no. 5, pp. 4931–4936, May 2022.

[8] I. Budihardjo et al., "Defining standard performance levels for power semiconductor devices[C]," in *Proc. IEEE Conf. 30th IAS Annu. Meeting Conf. Rec. Ind. Appl.*, 1995, vol. 2, pp. 1084–1090.

[9] C. L. Ma, P. O. Lauritzen, P.-Y. Lin, and I. Budihardjo, "A systematic approach to modeling of power semiconductor devices based on charge control principles," in *Proc. Power Electron. Specialist Conf.*, 1994, pp. 31–37.

[10] C. L. Ma, P. O. Lauritzen, P. Türkes, and H. J. Mattausch, "A physically-based Lumped-charge SCR model," in *Proc. IEEE Power Electron. Specialist Conf.*, 1993, pp. 53–59.

[11] C. L. Ma and P. O. Lauritzen, "A physics-based GTO model for circuit simulation," in *Proc. '95 - Power Electron. Specialist Conf.*, 1995, pp. 872–878.

[12] G. Birtek and A. B. Yıldız, "Analysis of switched capacitor circuits based on unified ideal switch model," in *Proc. 2nd Glob. Power, Energy Commun. Conf.*, 2020, pp. 98–101, doi: 10.1109/GPECOM49333.2020.9247910.

[13] G. Anand and A. K. Pandey, "Comparison and design of flyback converter using an ideal switch and a MOSFET switch," in *Proc. Int. Conf. Power Energy, Environ. Intell. Control*, 2018, pp. 589–593, doi: 10.1109/PEEIC.2018.8665449.

[14] H. Kuhn and D. Schrbder, "A new validated physically based IGCT model for circuit simulation of snubberless and series operation[C]," in *Proc. IEEE Ind. Appl. Conf.*, 2000, vol. 5, pp. 2866–2872.

[15] X. Wang, A. Caiafa, J. L. Hudgins, E. Santi, and P. R. Palmer, "Implementation validation a Phys.-based circuit model for IGCT with full Temp. dependencies[C]," in *Proc. IEEE Power Electron. Specialists Conf.*, 2004, vol. 1, pp. 597–603.

[16] X. Wang, J. L. Hudgins, E. Santi, and P. R. Palmer, "Destruction-Free parameter extraction for a physics-based circuit simulator IGCT Model[J]," *IEEE Trans. Ind. Appl.*, vol. 42, no. 6, pp. 1395–1402, Nov./Dec. 2006.

[17] G. Lyu et al., "Physics-based compact model of integrated gate commutated thyristor with multiple effects for high power Application," *IET Power Electron.*, vol. 11, 2018, pp. 1239–1247.

[18] S. Yin, Y. Gu, K. J. Tseng, J. Li, G. Dai, and K. Zhou, "A physics-based compact model of SiC junction barrier schottky diode for circuit simulation," *IEEE Trans. Electron Devices*, vol. 65, no. 8, pp. 3095–3103, Aug. 2018, doi: 10.1109/TED.2018.2840118.

[19] P. B. Vyas et al., "Reliability-Conscious MOSFET compact modeling with focus on the defect-screening effect of hot-carrier injection," in *Proc. IEEE Int. Rel. Phys. Symp.*, 2021, pp. 1–4, doi: 10.1109/IRPS46558.2021.9405197.

[20] N. Lophitis et al., "Experimentally validated three dimensional GCT wafer level simulations," in *Proc. 24th Int. Symp. Power Semicond. Devices ICs*, 2012, pp. 349–352.

[21] N. Lophitis et al., "The destruction mechanism in GCTs," *IEEE Trans. Electron Devices*, vol. 60, no. 2, pp. 819–826, Feb. 2013.

[22] T. K. Gachovska, *Modeling of Power Semiconductor Devices*. Lausanne, Switzerland: EPFL, 2012.

[23] X. Zhou, C. Zhuang, R. Zeng, C. Ren, C. Xu, and Z. Wang, "A one-dimensional physics-based compact model of reverse blocking IGCT devices," in *Proc. 11th Int. Conf. Power Energy Syst.*, 2021, pp. 321–326, doi: 10.1109/ICPES53652.2021.9683802.

Zhanqing Yu (Member, IEEE) was born in Inner Mongolia, China, in 1981. He received the B.Sc. and Ph.D. degrees in electrical engineering from Department of Electrical Engineering, Tsinghua University, Beijing, China, in 2003 and 2008, respectively.

After graduation, he became a Postdoctor, Lecturer, Associate Professor with the Department of Electrical Engineering, Tsinghua University, Beijing, China, in 2008, 2010, 2012, respectively. He has participated in projects sponsored by High-Tech R&D Program (863 Program), National Basic Research Program of China (973 Program), National Natural Science Foundation of China. His research interests include dc grid, dc breaker, electromagnetic environment, and electromagnetic compatibility.

Zongze Wang was born in Henan, China, in 1998. He received the B.S. degree in electrical engineering in 2012 from the Department of Electrical Engineering, Tsinghua University, Beijing, China, where he is currently working toward the Ph.D. degree in electrical engineering.

His current research interests include the high power electronic converter and HVdc transmission system.

Chaoqun Xu was born in Zhejiang, China, in 1996. He received the B.S. degree in electrical engineering in 2018 from the Department of Electrical Engineering, Tsinghua University, Beijing, China, where he is currently working toward the Ph.D. degree in electrical engineering.

His current research interests include the high power electronic converter, HVdc transmission system, and flexible dc distribution system.

Xuan Zhou was born in Hunan, China, in 1992. She received the B.S. and Ph.D. degrees in electrical engineering from the Department of Electrical Engineering, Tsinghua University, Beijing, China, in 2012 and 2017, respectively.

She was a Postdoctoral Researcher with the Department of Electrical Engineering, Tsinghua University in 2019. Her research interests include gas discharge, high voltage dc–ac transmission, plasma diagnostics, lightning physics, and Si-based semiconductor.

Zhengyu Chen was born in Tianjin, China, in 1992. He received the B.S. and Ph.D. degrees in electrical engineering from Tsinghua University, Beijing, China, in 2014 and 2019, respectively.

He was a Joint Postdoctoral Researcher with Tsinghua University and the University of Macau, Macau, China, in 2019. He is currently working at dc Research Center, Energy Internet Research Institute of Tsinghua University. His current research interests include power semiconductor devices and their gate unit drivers, HVdc systems, and dc circuit breakers.

Chunpin Ren was born in Zhejiang, China, in 1997. She received the B.S. degree in electrical engineering from the Department of Electrical Engineering, North China Electric Power University, Beijing, China, in 2019. She is currently working toward the Ph.D. degree in electrical engineering with the Department of Electrical Engineering, Tsinghua University, Beijing, China.

Her current research interests include high power semiconductor device manufacturing, modeling, and development.

Rong Zeng (Senior Member, IEEE) was born in Shaanxi, China, in 1971. He received the B.Eng., M.Eng., and Ph.D. degrees from the Department of Electrical Engineering, Tsinghua University, Beijing, China, in 1995, 1997, and 1999, respectively, all in electrical engineering.

He was a Lecturer, an Associate Professor, and Professor with the Department of Electrical Engineering, Tsinghua University, in 1999, 2002, and 2007, respectively. His research interests include air gap discharge, lightning protection, and electromagnetic compatibility in power systems, electric and magnetic field measurement by integrated electro-optical sensors, power semiconductor, HVdc system, and direct current circuit breaker.